Inhibition Effects on the Corrosion of Mild Steel in 1 M HCl by 1,1'-(2,2'-(2,2'-oxybis(ethane-2,1-diyl)bis(sulfanediyl)) bis(ethane-2,1-diyl))diazepan-2-one

A. Khadiri,[a] A. Ousslim,[a] K. Bekkouche,[a] A. Aouniti,[b] A. Elidrissi,[b] B. Hammouti[b,*]

[a] *LCSMA - Faculté des Sciences, Université Mohammed Premier, B.P. 717, 60000 Oujda, Morocco*
[b] *LCAE-URAC18, Faculté des Sciences, Université Mohammed Premier, B.P. 717, 60000 Oujda, Morocco*

Abstract

The inhibition of the corrosion of Mild Steel (MS) in 1 M HCl solution by a new synthesised organic compound, namely 1,1'-(2,2'-(2,2'-oxybis(ethane-2,1-diyl)bis (sulfanediyl))bis(ethane-2,1-diyl))diazepan-2-one, has been studied by weight loss measurements, electrochemical polarisation and electrochemical impedance spectroscopy (EIS). The experimental results have showed that this organic compound revealed a good corrosion inhibition and the inhibition efficiency is increased with the inhibitor concentration to reach 97% at 1 mM. Potentiodynamic polarisation suggested that it is a mixed type of inhibitor. EIS measurements show an increase of the polarisation resistance with the inhibitor concentration and the electrical equivalent circuit is determined. The inhibitor adsorption process on (MS) surfaces obeys the Langmuir adsorption isotherm and the adsorption isotherm parameters (K_{ads}, ΔG_{ads}, ΔH_{ads} and ΔS_{ads}) were determined. The temperature effect on the corrosion behaviour of (MS) in 1 M HCl without and with inhibitor at different concentration was studied in the temperature range from 308 to 353 K and the kinetic parameters activation such as E_a, ΔH_a and ΔS_a were evaluated.

Keywords: corrosion; inhibition; thermodynamic, adsorption, azepane.

Introduction

The corrosion of steel and ferrous alloys is a fundamental process playing an important role in economies and public safety [1]. Mild Steel is a well-known material used commonly in various industries. Acid solutions are often used for the removal of rust and scale in several industrial processes. In this case,

---

* Corresponding author. E-mail address: hammoutib@gmail.com

hydrochloric acid is one of the most widely used agents. Various types of organic compounds are widely used as corrosion inhibitors for protection of materials against deterioration from corrosion [2-14].A persuade of the literature on acid corrosion inhibitors reveals that most organic substances employed as corrosion inhibitors act by adsorption on the metal surface. The adsorption of the inhibitors mainly depends on the presence of π-electrons and heteroatoms such as nitrogen, oxygen, phosphorus and sulphur, which are considered as adsorption centres [15-17].

In this work, we investigate the corrosion of (MS) in 1 M HCl by 1,1'-(2,2'-(2,2'-oxybis(ethane-2,1-diyl)bis(sulfanediyl))bis(ethane-2,1-diyl))diazepan-2-one (AZEPE). Weight loss tests and electrochemical techniques such as potentiodynamic polarisation and electrochemical impedance spectroscopy have been used to study the effect of addition of this compound on the corrosion of steel in hydrochloric acid solution.

Experimental

Inhibitor

A mixture of N-vinyl caprolactame (27.84 g, 0.2 mol) and 2, 2-azo-bis-isobutyronitrile (AIBN) (0.082g, 5×10^{-4} mol) in 100 mL of acetonitrile (CH_3CN) was added drop by drop during 30 min to 2-mercaptoethylether dissolved in 50 mL of acetonitrile. Then, the mixture was stirred during 3h in the presence of pure nitrogen (N_2) at 70 °C under atmospheric pressure. The solvent and the excess of 2-mercaptoethylether were removed and the product was purified by chromatographic on a silica column (eluent CH_2Cl_2), to give AZEPE product as yellow oil, yield 90%. A schematic representation of the synthesis is shown in Fig. 1. This inhibitor was synthesized according to A. Ousslim in our laboratory and characterised by ^{1}H-NMR, ^{13}C-NMR and IR spectroscopy. **^{1}H-NMR** (CDCl$_3$, δ (ppm)): 1.29 (m, 2H); 1.55 (m, 2H); 1.57 (t, 2H); 2.18 (t, 2H); 2.61(t, 2H); 2.70(t, 2H) ; 3.2 (t, 2H) ; 3.65 (t, 2H) ; 3.74 (t, 2H) ;**^{13}C-NMR** (CDCl$_3$, δ (ppm)): 23.5; 29.9; 30.8; 31.7; 37.26; 44.12; 49.8, 72.2, 174.28; **IR** (KBr, ν (cm^{-1})): 2918 (FF); 2864 (m); 1656-1624 (FF); 1463(f); 1308 (f); 1197 (f); 1113 (FF); 1093 (f); 725 (f).
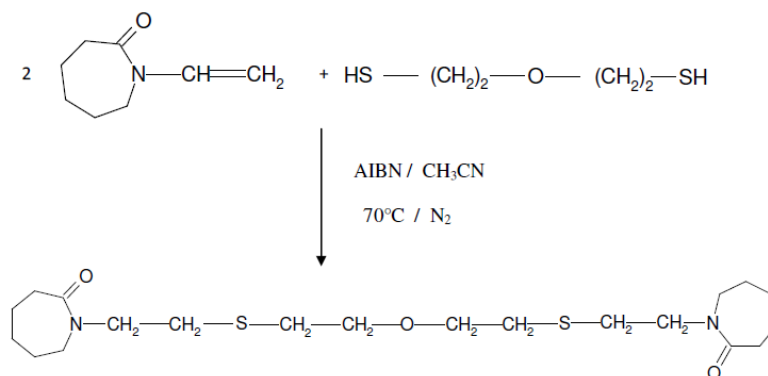
Figure 1. Structure and synthetic route of 1,1'-(2,2'-(2,2'-oxybis(ethane-2,1-diyl)bis(sulfanediyl))bis(ethane-2,1-diyl))diazepan-2-one(AZEPE).

Materials

Mild steel sheets used in this study contain 0.21% C, 0.38% Si, 0.05% Mn, 0.05% S, 0.09% P, 0.01% Al and the remainder iron (Fe). The steel specimens used were pre-treated prior to the experiment by grinding with emery paper (grade 400, 600 and 1200), then rinsed with bi-distilled water, degreased, dried and immersed in the corrosive solution.

Weight loss studies

Weight loss measurements were performed at 308 K (except for temperature effect) for 6 h by immersing the mild steel specimens into non-de-aerated solution (50 mL) without and with various concentrations of the inhibitor. After immersion period, the steel specimens were taken out, washed, dried and weighted by an analytical balance (precision± 0.1 mg); three experiments were performed in each case and the mean value of the weight loss is calculated.

Electrochemical measurements

Electrochemical measurements were performed in a conventional three-electrode cylindrical pyrex glass cell. The temperature is controlled at 308 ± 1 K. The working electrode (WE) in the form of disc is cut from steel, has a geometric area of 1 cm^2 and is embedded in polytetrafluoroethylene (PTFE). A saturated calomel electrode (SCE) and a platinum electrode are used, as reference and auxiliary electrodes, respectively. The electrochemical measurements were carried out using Tacussel Radiometer PGZ 100, which was controlled by a personnel computer. Before each experiment, the work electrode was allowed to corrode freely for 1 h (no de-aeration, no stirring). All EIS were recorded at the open circuit potential E_{OCP}. The duration of one EIS experiment was about 20 min. The response of the electrochemical system to ac excitation with a frequency ranging mainly from 100 kHz to 10 mHz and peak to peak amplitude of 10 mV was measured with data density of 10 points per decade. The impedance data were analyzed and fitted with the simulation ZView 2.8 equivalent circuit software.

The polarisation measurements were recorded after the EIS measurements on the same electrode without any further surface treatment. Before and during each experiment, the test solutions were stirred by the magnetic stirrer and de-aerated in the cell by using pure nitrogen. The polarisation curves were obtained potentiodynamically between -800to -200mV (Ag/AgCl) with the scan rate of 1 mV s^{-1}.

Results and discussions
Weight loss measurements
Effect of inhibitor concentration

The effect of addition of the inhibitor tested at different concentrations on the corrosion of mild steel in 1 M HCl solution is studied by weight loss at 308±1K after 6 h of immersion period. For every concentration of inhibitor, the mean

value of the corrosion rate W_{corr} (mg cm^{-2} h^{-1}) was determined and the inhibitor efficiency, $E_W(\%)$, was calculated using equations (1) and (2), respectively.

$$W_{corr} = \frac{m_b - m_a}{S \times t} \tag{1}$$

$$Ew(\%) = \left(1 - \frac{W_{corr}}{W_{corr}^\circ}\right) \times 100 \tag{2}$$

where m_b and m_a are the mass of the specimen before and after immersion in the tested solution, W_{corr} and W_{corr}° are the corrosion rates of mild steel in inhibited and uninhibited solution, respectively, S is the area of the mild steel specimen (cm^2) and t is the immersion time (h).

The results obtained are summarized in Table 1.

It is very clear that the corrosion rate (W_{corr}) decreases with increasing inhibitor concentration and the inhibition efficiency increases with inhibitor concentration and attains *95.56% at 1mMof inhibitor.*

Table 1. Corrosion parameters obtained from weight loss measurements for mild steel in 1 M HCl containing various concentrations of the inhibitor at 308 K.

C(mM)	W_{corr}(mg cm^{-2} h^{-1})	$E_w(\%)$
Blanc	2.030	-
0.001	0.965	52.5
0.005	0.428	78.9
0.01	0.270	86.7
0.05	0.128	93.7
0.1	0.106	94.8
0.5	0.104	94.9
1	0.090	95.6

Table 2. Effect of temperature on the corrosion rate of mild steel in 1 M HCl at different concentrations in the temperature range 308-353 K for 2 h.

C (mM)	Blank	0.05		0.1		0.5		1	
T (K)	W_{corr}^0 (mg cm^{-2} h^{-1})	W_{corr}^0 (mg cm^{-2} h^{-1})	Ew (%)	W_{corr}^0 (mg cm^{-2} h^{-1})	Ew (%)	W_{corr}^0 (mg cm^{-2} h^{-1})	Ew (%)	W_{corr}^0 (mg cm^{-2} h^{-1})	Ew (%)
308	1.73	0.178	89.7	0.136	92.1	0.083	95.2	0.074	95.7
313	2.43	0.237	90.2	0.215	91.1	0.166	93.1	0.099	95.9
323	5.58	0.544	90.7	0.557	90.5	0.358	93.9	0.237	95.9
333	12.11	1.24	89.7	1.11	90.9	0.756	93.7	0.56	95.4
343	26.11	7.12	72.7	3.93	84.9	3.63	86.9	2.32	91.1
353	46.23	28.37	39.4	19.19	58.5	7.00	84.8	6.22	86.5

Effect of temperature

The effect of temperature on the inhibition efficiency, in the temperature range 308-353 K, in 1 M HCl, was studied using gravimetric experiments in the absence and presence of 0.05, 0.1, 0.5 and 1 mM of inhibitor after 2 h of immersion time. The results obtained are summarized in Table 2.

We note a slight variation in the inhibition efficiency at all concentrations for inhibitor studies in the temperature range 308 – 353 K. In addition, the inhibition efficiency is quietly independent of the temperature in the range 308-333 K.

Adsorption isotherm

It is universally accepted that the organic inhibitors act by means of physiadsorption or chemiadsorption on the metal surface. Isotherm equations are frequently used to describe the adsorption. In order to gain more information about the mode of adsorption of the inhibitor on the surface of mild steel, the experimental data have been tested with several adsorption isotherms. The values of surface coverage (Θ) for different concentrations at different temperatures have been used to explain the best isotherm that determines the adsorption process. The values of surface coverage (Θ) were evaluated from weight loss measurements by using the following equation:

$$\theta = \frac{W_{corr}^{\circ} - W_{corr}}{W_{corr}} \quad (3)$$

In this equation, W_{corr} and W_{corr}° represent the corrosion rates of mild steel in the presence and absence of the inhibitor, respectively. The correlation of with concentration of inhibitor was evaluated by different adsorption isotherms such as Langmuir, Frumkin and Temkin. However, the best fit was obtained from the Langmuir isotherm (Fig.2). These isotherms are given by equations (4), (5) and (6), respectively [18-20].

$$\frac{C}{\theta} = \frac{1}{K_{ads}} + c \quad (4)$$

$$\theta = \frac{1}{f} \ln \left(K_{ads} \frac{C(1-\theta)}{c} \right) \quad (5)$$

$$\theta = \frac{1}{f} \ln (K_{ads} \, C) \quad (6)$$

where K_{ads} is the equilibrium adsorption and f is the molecular interaction constant.

The equilibrium constant for adsorption process is related to the free energy of adsorption, ΔG_{ads}, and is expressed by equation (7)

$$K_{ads} = \frac{1}{55.55} exp \left(-\frac{\Delta G_{ads}}{R \times T} \right) \quad (7)$$

where 55.55 is the molar concentration of water in the solution expressed in (mol l^{-1}); R is the gas constant (8.314 J K^{-1} mol^{-1}) and T is the absolute temperature (K).The heat of adsorption ΔH_{ads} is obtained from the Van't Hoff's equation (eq. 8) [21,22]. When LnK_{ads}vs. (1/T) is plotted (Fig. 3), the value of ΔH_{ads} is obtained from the slope and ΔS_{ads} is obtained for a range of temperatures with equation (9):

$$LnK_{ads} = -\frac{\Delta H_{ads}}{R \, T} + constant \quad (8)$$

$$\Delta G_{ads} = \Delta H_{ads} - T \Delta S_{ads} \quad (9)$$

The values of $K_{ads}, \Delta G_{ads}, \Delta H_{ads}$ and ΔS_{ads} are disclosed in Table 3. The negative values of ΔG_{ads} along with high K_{ads} indicate a spontaneous adsorption process [23, 24]. Generally, the ΔG_{ads} values up to -20 kJ mol^{-1} are consistent with the electrostatic interaction between the charged molecules and the charged

metal (physisorption). On the other hand, negative values less than -40 kJ mol^{-1} involve sharing or transferring of electrons from the inhibitor molecules to the metal surface to form a co-ordinate type of band (chemisorption) [25]. The calculated ΔG_{ads} values are ranging between -41.07 and -43.85 kJ mol^{-1}, suggesting that the inhibitor was adsorbed chemically onto the mild steel surface. The higher values of K_{ads} and ΔG_{ads} refer to higher adsorption and higher inhibiting effect [26]. The negative value of ΔH_{ads} also shows that the adsorption of the inhibitor is an exothermic process [27]. The adsorption of inhibitor molecules is accompanied by negative values of ΔS_{ads} because of the confining of an adsorbed molecule to a thin surface layer (certain degrees of freedom are lost) [28].
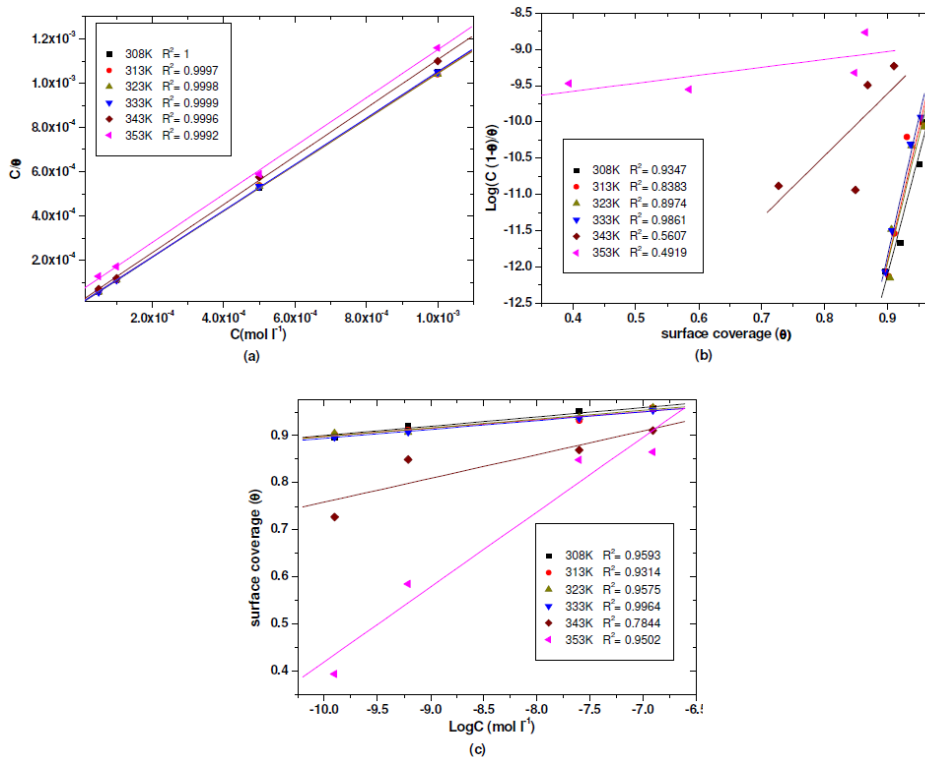
Figure 2. Different adsorption isotherm plots for the adsorption in different temperatures of the inhibitor in 1 M HCl on the surface of mild steel. (a) Langmuir's isotherm, (b) Frumkin's isotherm and (c) Temkin's isotherm.
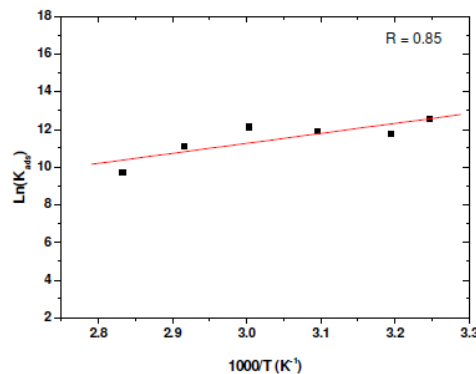
Figure 3. Vant Hoff's plot for MS in 1 M HCl in presence of the inhibitor.

Table 3. Thermodynamic parameters for the adsorption of the inhibitor in 1 M HCl at different temperatures.

Temperature (K)	K_{ads} (M^{-1})	ΔG_{ads} (kJ mol^{-1})	ΔH_{ads} (kJ mol^{-1})	ΔS_{ads} (J K^{-1} mol^{-1})
308	280963.59	-42.41	-44.96	-5.5
313	129058.24	-41.08		-9.66
323	143970.65	-42.68		-4.41
333	182355.97	-43.85		-0.76
343	64650.02	-43.04		-3.10
353	15972.42	-40.19		-11.09

Activation parameters

Kinetic model can be used to explain the inhibitor behaviour. The apparent activation energy for the corrosion process was calculated from the Arrhenius equation:

$$Ln(W_{corr}) = -\frac{E_a}{R \times T} + Ln(A) \quad (10)$$

where E_a represents the apparent activation energy, A is the pre-exponential factor and W_{corr} is the corrosion rate. Fig 4.a shows the Arrhenius plot of Log (W_{corr}) vs. $\frac{1}{T}$ in the absence and presence of different concentrations of the inhibitor at different temperatures. The enthalpy of activation ΔH_a and entropy of activation ΔS_a were obtained from the transition state equation:

$$W_{corr} = \frac{R \times T}{N_A \times h} \exp\left(\frac{\Delta S_a}{R}\right) \exp\left(-\frac{\Delta H_a}{R \times T}\right) \quad (11)$$

where h is the Plank's constant, N_A is the Avogadro's number, T is the absolute temperature and R is the universal gas constant. Straight lines of $Log\left(\frac{W_{corr}}{T}\right)$ against $\frac{1}{T}$ are plotted in Fig.4b; ΔH_a and ΔS_a are obtained from the slope and intercept of the linear plots, respectively. The values Ea, ΔH_a and ΔS_a at different temperatures are presented in Table 4. We note that the linear regression coefficients are over 0.97 indicating the validation of the employed kinetic model.
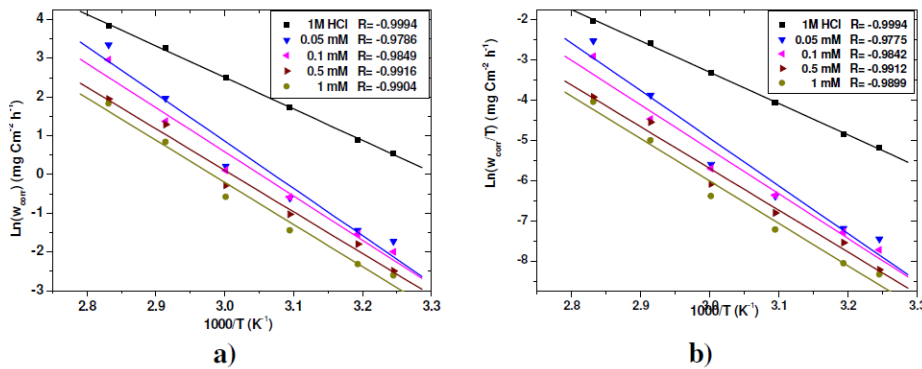
Figure 4. a) Arrhenius plots for mild steel in 1 M HCl without and with different concentrations of inhibitor. b) Transition state plots for mild steel in 1 M HCl without and with different concentrations of inhibitor.

According to the report in literature [29, 30], higher value of E_a was considered as physiadsorption. Because the electrochemical corrosion is relevant to heterogeneous reaction, the pre-exponential factor A in the Arrhenius equation is related to the number of active centres with different E_a on the metal surface: (i) the activation energy in the presence of the inhibitor is lower than that of pure acidic medium, namely $E_a(inh) < E_a(HCl)$, which suggests a smaller number of more active sites remaining uncovered in the corrosion process, (ii) the activation energy in the presence of the inhibitor is higher than that of pure acidic medium, $E_a(inh) > E_a(HCl)$, which represents the inhibitor adsorbed on most active adsorption sites (having the lowest energy) and the corrosion takes place chiefly on the active sites (having the higher energy).

Table 4. Values of activation thermodynamic parameters for mild steel dissolution in 1 M HCl in the absence and presence of different concentrations of the inhibitor.

C(mM)	Ea (kJ mol^{-1})	A	ΔH_a (kJ mol^{-1})	ΔS_a (J mol^{-1} K^{-1})
Blanc	67.54	4.74×10^{11}	64.80	-30.52
0.05	101.26	1.78×10^{16}	98.52	56.99
0.1	94.73	1.28×10^{15}	91.99	35.12
0.5	89.08	1.03×10^{14}	86.34	14.20
1	90.36	1.20×10^{14}	87.62	15.47

The data in Table 4 specifically indicate that the values of E_a in presence of the inhibitor are larger than that in the absence of the inhibitor, which is consistent with the latter mentioned above; this means that the adsorbed inhibitor molecules block the most active sites, while the sites of higher activation energy, which are greater in number, take part in the subsequent corrosion [29, 31]. The positive values of ΔH_a manifest the endothermic nature of the dissolution process; ΔS_a was also positive in the presence of the inhibitor, suggesting that active complexes were formed by the substitution of water for the inhibitor.

This part showed that physical adsorption is not neglected and the mechanism of inhibition may be endorsed that inhibition of inhibitor acted both by physical and chemical adsorption.

Inspection of the data reveals that the ΔH_a values for dissolution reaction of mild steel in 1 M HCl in the presence of inhibitor are higher (86.34; 98.52 kJ mol^{-1}) than that of in the absence of inhibitor (64.8 kJ mol^{-1}). The positive signs of ΔH_a reflect the endothermic nature of mild steel dissolution process, which suggests the slow dissolution of mild steel in presence of the inhibitor [32]. In the presence of inhibitor, one can notice the E_a and ΔH_a values vary in the same way (Table 4). These results permit to verify the known thermodynamic relation between the Ea and ΔH_a (ΔH_a = Ea - TΔS_a) [33,34].

Potentiodynamic polarisation

The values of corrosion potential E_{corr}, corrosion current density i_{corr}, and anodic and cathodic slopes (β_a and β_c) can be evaluated from anodic and cathodic regions of Tafel plots. The linear Tafel segments of anodic and cathodic curves were extrapolated to corrosion potential to obtain corrosion current densities (i_{corr}).
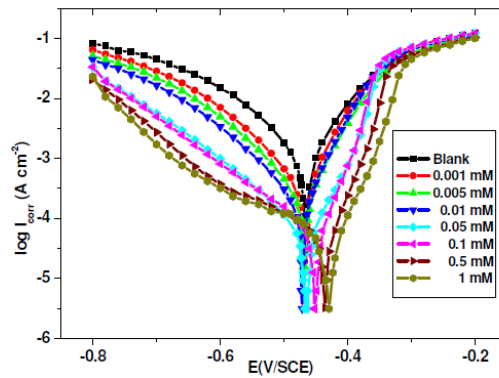
Figure 5. Potentiodynamic polarisation curves for mild steel in 1 M HCl without and with different concentrations of the inhibitor.

The inhibition efficiency was evaluated from the measured i_{corr} values using the relationship

$$E(\%) = \frac{i_{corr}^{0} - i_{corr}}{i_{corr}^{0}} \times 100 \quad (12)$$

where i_{corr}^{0} and i_{corr} are the values of corrosion current density in absence and presence of the inhibitor, respectively.

Fig. 5 shows the polarisation curves recorded on mild steel in 1 M HCl solutions in the absence and presence of different concentrations of the inhibitor. It can be seen from this figure that with the increase of inhibitor concentration, both anodic and cathodic reactions were supported through inhibitor adsorption on the mild steel surface in 1 M HCl solution.

Table 5 shows that the i_{corr} decreases with the increase in inhibitor concentration and the inhibition efficiency reaches to the maximum at 1 mM of inhibitor. From this table, it is also clear that E_{corr} values do not shift with inhibitor concentration. In literature, it has been reported that if the displacement in E_{corr} is > 85 mV with respect to E_{corr}, the inhibitor can be seen as of the cathodic or anodic type, and if the displacement in E_{corr} is < 85 mV, the inhibition can be seen as of the mixed type [35-37]. In our study the maximum displacement in E_{corr} value was 37 mV towards anodic region, which indicates that the inhibitor is of the mixed type with predominance of the anodic type. The values of the slopes of the anodic Tafel lines, β_a, are lower than those for uninhibited solution, which suggests that the inhibitor can affect the kinetics of the anodic process. The inhibition efficiencies calculated from potentiodynamic polarisation curve are in good agreement with those obtained from weight loss measurements.

Electrochemical impedance spectroscopy (EIS) measurements
The corrosion behaviour of MS in 1 M HCl solution in the absence and presence of various concentrations of the inhibitor after immersion for 1 h at 308 K was investigated using EIS. In general, kinetic information of the electrode interface between the mild steel and the test solution can be obtained from the shape of the impedance diagrams [38]. The recorded EIS spectrum for MS in 1 M HCl solution in absence and presence of different concentrations (except 0.5 and 1 mM) (Fig.6) shows a depressed capacitive loop in the high frequency (HF) range and an inductive loop in the lower frequency (LF) range. The HF capacitive loop

can be attributed to the charge transfer reaction and time constant of the electric double layer and to the surface non-homogeneity of interfacial origin, such as those found in adsorption process on metal surface, and the LF inductive loop may be attributed to the relaxation process like Cl^-_{ads} and H^+_{ads} on working electrode surface [39]. For the concentration 0.5 and 1mM, Fig.6 shows only one depressed capacitive loop.

Table 5. Polarisation parameters and the corresponding inhibition efficiency for corrosion of mild steel in 1M HCl solution containing different concentrations of inhibitor.

C (mM)	E_{corr} (mV)	i_{corr} (mA cm^{-2})	β_a (mV dec^{-1})	βc (mV dec^{-1})	E_i (%)
Blanc	-467.3	0.966	71.1	-101	-
0.001	-469.8	0.372	55.5	-98.1	61.5
0.005	-470.0	0.224	55.2	-90.6	76.8
0.01	-473.6	0.213	52.8	-104.7	77.9
0.05	-467.4	0.047	55.9	-93.7	95.1
0.1	-452.7	0.036	38.9	-90.6	96.2
0.5	-437.2	0.035	41.4	-135.1	96.3
1	-430.0	0.030	47.8	-130.6	96.9

The diameters of capacitive loops increase with the increase in inhibitor concentration, which indicates the increase of charge transfer and improvement in inhibiting effect on MS corrosion (Fig.6). It reveals that the presence of the inhibitor in 1 M HCl solutions increases the charge transfer resistance due to the formation of a protection layer on the MS surface, but it does not change other aspects of the corrosion behaviour. These results agree with those of polarization measurements, that is, the inhibitor does not substantially alter the electrochemical reactions mechanism. The above observation is also verified by the Bode plots (Fig. 6). Each Bode-phase diagram consists of a single wave crest and a portion of curve under the zero phase degree. However, it is clear that the shapes of the impedance plots for the inhibited electrodes are not essentially different from those of the uninhibited electrodes. Electrical equivalent circuits are generally used to model the electrochemical behaviour and to calculate the impedance parameters [40].
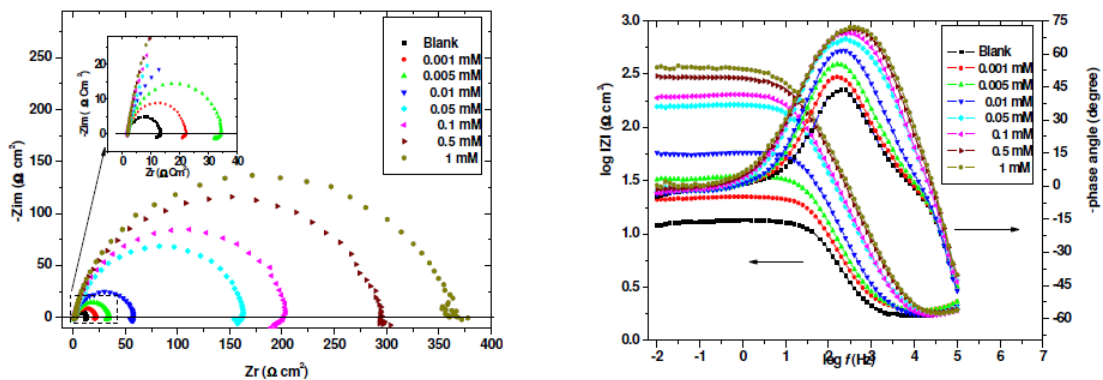
Figure 6. Nyquist and Bode-phase diagrams for mild steel in 1 M HCl containing different concentrations of inhibitor at 308 K.

(a)   (b)
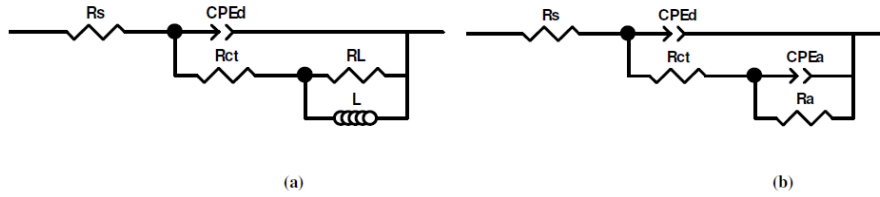
Figure 7. Electrical equivalent circuit used for modelling the interface mild steel / 1 M HCl solution without and with inhibitor.

Figs.7a & b show the equivalent circuit model used to fit the experimental impedance data of MS in 1 M HCl in absence and presence of different concentrations (except 0.5 and 1 mM). In this case the addition of inhibitor has no effect on the shape of the impedance spectra; two equivalent circuits may be proposed to fit these systems that charge transfer controls the corrosion process. The same equivalent circuit was often used to describe the corrosion inhibition caused by organic compounds in acidic medium [41-46].
In the equivalent circuit R_s is the solution resistance, CPE_d is a constant phase element, R_{ct} is the charge transfer resistance, L is the inductance and $R_{ct}+ R_L$ presents the polarisation resistance (R_P). Resistance R_L and inductance L may be correlated with a slow frequency intermediate process [47]. The presence of inductance L in the impedance spectra indicates that the MS is still dissolved by the direct charge transfer in the presence of the inhibitor [45]. The constant phase element, CPE, is introduced in the circuit instead of a pure double layer capacitor in order to take into account the electrode surface heterogeneity resulting from surface roughness, impurities, dislocations, grain boundaries, adsorption of inhibitors, formation of porous layers [31,48] and therefore to give a more accurate fit [49]. The impedance of the CPE is expressed as:

$$Z_{CPE} = \frac{1}{A(iw)^n} \quad (13)$$

where A is the proportionality of CPE (in $\Omega^{-1}s^n$ cm^{-2}), ω is the sine wave modulation angular frequency (in rad s^{-1}), $i^2 = -1$ is the imaginary number, and n is an empirical exponent which measures the deviation from the ideal capacitive behaviour [50,51]. The CPE can be expressed by the values of n if resistance (n = 0, A = R), capacitance (n = 1, A = C), Inductance (n = -1, A = L) and Warburg impedance (n = 0.5, A = W) [52]. The experimental data were very well fitted according to the proposed equivalent circuit and as an example; the simulated curves are presented in Fig. 8. The corresponding fitting results are listed in Table 6. In this table are also shown the calculated double layer capacitance (C_{dl}) derived from the CPE_d parameters according to equation (14) [53]; the relaxation time constant (τ_d) of charge-transfer process was calculated using equation (15) [53]:

$$C_{dl} = (A_d(R_{ct})^{1-n_d})^{1/n_d} \quad (14) \qquad \tau_d = C_{dl} \times R_{ct} \quad (15)$$
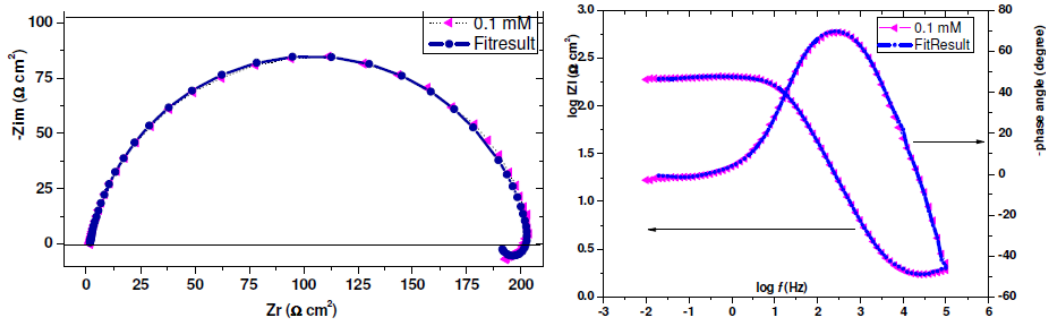
Figure 8. EIS Nyquist and Bode-phase diagram for mild steel / 1 M HCl + 0.1 mM of inhibitor interface using structural model in Fig. 7a.

Results in Table 6 show that R_{ct} value increased with the concentration of the inhibitor. In addition, the value of proportional factor A of CPE varies in a regular manner with inhibitor concentration. The change in the values of R_{ct} and A can be related to the gradual removal of water molecules by AZEPE molecules on the electrode surface and consequently leads to decrease in the number of active sites necessary for the corrosion reaction [54].

The value of the relaxation time constant (τ_d) slowly increases with AZEPE concentration as well and the time of adsorption process becomes therefore much higher, which means a slow adsorption process [55]. This shows that there is an agreement between the amount of charge that can be stored (that is capacitance) and discharge velocity in the interface (τ_d) [56]. At LF region, the inductance (L) increases with inhibitor concentration.

Table 6. Impedance parameters and inhibition efficiency values for mild steel after 1 h immersion period in 1 M HCl containing different concentrations of AZEPE at 308 K.

C (mM)	R_s (Ω cm^2)	$10^6 A_d$ (Ω^{-1}s^n cm^{-2})	n_d	R_{ct} (Ω cm^2)	C_{dl} (μF cm^{-2})	τ_d (ms)	R_L (Ω cm^2)
Blanc	1.705	385.69	0.906	10.03	217.34	2.18	1.63
0.001	1.954	306.04	0.895	18.8	167.10	3.14	1.69
0.005	1.939	237.67	0.895	30.21	133.21	4.02	3.04
0.01	1.781	153.24	0.897	52.81	88.14	4.65	4.53
0.05	1.805	94.39	0.867	155.7	49.40	7.69	9.78
0.1	1.695	74.54	0.886	189.2	43.08	8.15	13.80
0.5	1.892	40.51	0.917	181.6	25.97	4.72	-
1	1.885	34.78	0.919	200.2	22.45	4.49	-

C (mM)	L (H cm^{-2})	$10^6 A_a$ (Ω^{-1}s^n cm^{-2})	n_a	R_a (Ω cm^2)	C_a (μF cm^{-2})	τ_a (ms)	R_p (Ω cm^2)	E_Z (%)
Blanc	12.72	-	-	-	-	-	11.74	-
0.001	4.38	-	-	-	-	-	20.75	43.5
0.005	2.31	-	-	-	-	-	32.15	63.5
0.01	3.50	-	-	-	-	-	54.59	78.5
0.05	7.20	-	-	-	-	-	157.51	92.6
0.1	22.72	-	-	-	-	-	190.90	93.8
0.5	-	209.14	0.705	112.17	43.50	4.88	295.66	96.0
1	-	209.84	0.671	163.3	40.19	6.56	365.39	96.8

The related inhibition efficiency, E_Z(%), is calculated from $R_P = (R_{ct}+R_L)$ using the following equation (16):

$$E_z(\%) = \frac{R_p - R_p^\circ}{R_p}(16)$$

where R_p° and R_p are the ac polarisation resistance of mild steel electrode in the uninhibited and inhibited solutions, respectively.

The equivalent circuit for the concentrations 0.5 and 1 mM of inhibitor is shown in Fig 7.b. In this model R_s refers the solution resistance, R_{ct} the charge transfer resistance, CPE_d the constant phase element of the high frequency semicircle that can be attributed to the charge transfer process, R_a the resistance of the adsorbed inhibitor, CPE_a the constant phase element of the inhibitor film due to the inhibitor's adsorption on the steel surface, and the sum $R_{ct} + R_a$ presents the polarisation resistance R_P. The same equivalent circuit was often used to describe the corrosion inhibition caused by organic compounds in acidic medium [1, 53,57-58]. The time constant of the adsorption process is $\tau_a = R_a\,C_a$, the adsorption capacitance being again replaced by a CPE, and C_a is calculated by equation (17).

$$C_a = \left(A_a (R_a)^{1-n_a}\right)^{1/n_a} \quad (17)$$

The experimental data were very well fitted according to the proposed equivalent circuit and as an example; the calculated curves are presented in Fig. 9. The main fitted parameters are summarised in Table 6. From these results, it's clear that R_{ct} increase and C_{dl} decrease with inhibitor concentration. A large R_{ct} is associated with a slower corroding system [48, 59]. Furthermore, the decrease in the C_{dl} with increase in inhibitor concentrations may be attributed to the formation of a protective layer on the mild steel surface [60].The increase of the n_d values after addition of AZEPE in 1 M HCl solution (0.917–0.919) when compared to that obtained in uninhibited solution (0.889) can be explained by some decrease of the initial surface heterogeneity, due to the adsorption of the inhibitor on the most active adsorption sites on the steel surface[48]. In the same way, the values of the adsorption time constant τ_a show a marked tendency to increase with concentration and they are higher than τ_d; the apparent increase of τ_a with concentration is influenced by the adsorption process. The values of n_a are lower than those of n_d, indicating greater energy distribution in the adsorption layer [53]. The resistance values R_a are lower than R_{ct} values, so the total resistance R_P is dominated by R_{ct} and increases significantly with the inhibitor concentration.
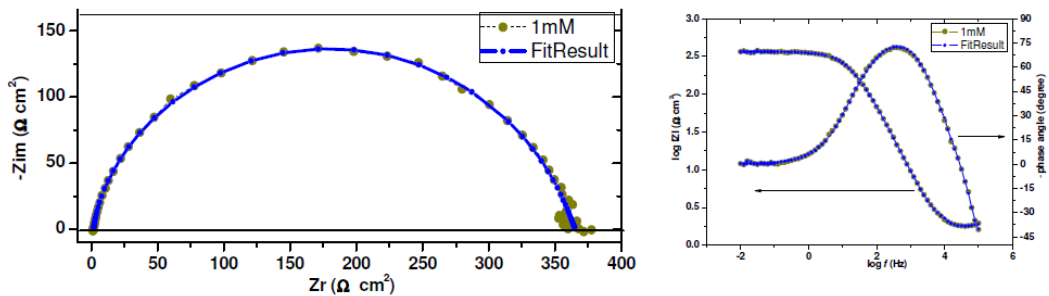
Figure 9. EIS Nyquist and Bode-phase diagram for mild steel / 1 M HCl + 1 mM of inhibitor interface using structural model in Fig. 7b.

The related inhibition efficiency, $E_Z(\%)$, is calculated from $R_P = (R_{ct}+R_a)$ using eq (16). It is obvious that the increase in inhibitor concentration enhances R_P, and consequently improves the inhibition efficiency till reaching their maximum value at 1 mM (R_P = 365.39 Ω cm^2, $E_Z(\%)$ = 96.76) The inhibition efficiency calculated by EIS shows the same trend as those obtained from the weight loss measurements and the potentiodynamic polarisation methods.

Conclusions

The principal findings of the present work can be summarised as follows:

The compound 1,1'-(2,2'-(2,2'-oxybis(ethane-2,1-diyl)bis(sulfanediyl))bis(ethane-2,1-diyl))diazepan-2-one, is a good inhibitor for steel in 1 M HCl.

The adsorption of the inhibitor obeys the Langmuir adsorption isotherm. The high value of adsorption equilibrium constant and negative value of free energy of adsorption suggested that the inhibitor is strongly adsorbed on MS surface.

The temperature effect reveals that the AZEPEis a good inhibitor at high temperature.

The polarisation measurements reveal that AZEPEbehaves as a mixed type inhibitor by inhibiting both anodic metal dissolution and cathodic hydrogen evolution reactions.

Data obtained from electrochemical impedance spectroscopy (EIS) technique show an increase of the polarisation resistance (R_P) and a decrease of the capacitance values with the concentration of the inhibitor. Both double layer and adsorption capacitances are distributed and therefore modelled by constant phase elements (CPE) due to the surface inhomogeneity.

Values of the corrosion inhibition efficiency, determined by weight loss, potentiodynamic polarisation and EIS measurements are in reasonable agreement.

References
1.   Doner A, GulfezaKardas. Corros Sci 2011;53:4223.
2.   Bentiss F, Traisnel M, Lagrenee M. Corros Sci. 2000;42:127.
3.   Pillali C, Narayan R.Corros Sci. 1983;23:151.
4.   Growcock F, Lopp VR, Corros Sci. 1988;28:397.
5.   Bekkouch K, Aouniti A, Hammouti B, et al. J Chim Phys. 1999;96:838.
6.   Kertit S, Bekkouche K, Hammouti B, Rev Métall. 1998;95: 251.
7.   Bouzidi D, Kertit S, Hammouti B, et al. J ElectrochemSoc India 1997;46:23.
8.   Kertit S, Hammouti B, Taleb M, et al. Bull Electrochem. 1997;13:241.
9.   Hammouti B, Melhaoui A, Kertit S. Bull Electrochem. 1997;13:97.
10.   Touhami F, Aouniti A, Kertit S, et al. Corros Sci. 2000;42:929.
11.   Touhami F, Hammouti B, Aouniti A. Ann Chim Sci Mat. 1999;24:581.
12.   Aouniti A, Hammouti B, Brighli M, et al. J Chim Phys. 1996;93:1262.
13.   Hammouti B, Aouniti A, Taleb M, et al. Corrosion. 1995;51:411.
14.   Aouniti A, Hammouti B, Kertit S. Bull Electrochem. 1998;14:193.

15. Avci G. Mater Chem Phys. 2008;112:234.
16. Avci G. Colloids Surf A: Physicochem Eng Asp. 2008;317:730.
17. Doner A, Solmaz R, Ozcan M, et al. Corros Sci. 2011;53:2902.
18. Bayol E, Kayakırılmaz K, Erbil M. Mater Chem Phys. 2007;104:74.
19. Frumkin AN. Prog. Surf Sci. 1977;8:1.
20. Durnie W, Marco RD, Jefferson A, et al. J Electrochem Soc. 1999;146:1751.
21. Zhao TP, GN Um. Corros Sci. 1999;41:1937.
22. Tang L, Mu G, Liu G. Corros Sci. 2003;45:2252.
23. Scendo M. Corros Sci. 2007;49:373.
24. Soltani N, Behpour M, Ghoreishi SM, et al. Corros Sci. 2010;52:1351.
25. Bouklah M, Hammouti B, Lagrenee M, et al. Corros Sci. 2006;48:2831.
26. Solmaz R, G Kardas, Culha M, et al. Electrochim Acta. 2008;53:5941.
27. Gomma MK, Wahdan MH. Mater Chem Phys. 1995;39:209.
28. Do DD. Adsorption Analysis: Equilibria & Kinetics. London: Imperial College Press;1998.
29. Chen W, Luo HQ, Li NB. Corros Sci. 2011;53: 3356.
30. Tu S, Jiang X, Zhou L, et al. Corr Sci. 2012;65:13.
31. Popova A, Sokolova E, Raicheva S. et al. Corros Sci. 2003;45:33.
32. Guan NM, Xueming L, Fei L. Mater Chem Phys. 2004;86:59.
33. Ahamad I, Prasad R, Quraishi MA. Corros Sci. 2010;52:933.
34. Yadav DK, Quraishi MA, Maiti B. Corros Sci. 2012;55:254.
35. Ashassi-Sorkhabi H, Majidi MR, Seyyedi K. Appl Surf Sci. 2004;225:176.
36. Riggs Jr OL. Corrosion Inhibitors. 2nd ed. Houston, TX;1973.
37. Behpour M, Ghoreishi SM, Mohammadi N, et al. Corros Sci. 2010;52:4046.
38. Lorenz WJ, Mansfeld F. Corros Sci 1981;21: 647.
39. Ahamad I, Prasad R, Quraishi MA. Corros Sci. 2010;52: 933.
40. Macdonald JR. Electroanal Chem. 1987;223: 25.
41. Khaled KF, Amin MA. Corros Sci. 51 2009; 1964.
42. Amin MA, Ibrahim MM. Corros Sci. 53 2011; 873.
43. Hermas AA, Morad MS, Wahdan MH. Appl Electrochem. 2004;34:95.
44. Poornima T, Jagannatha N, Shetty AN. Port Electrochim Acta. 2010;28:173.
45. Zarrok H, Zarrouk A, Hammouti B, et al. Corros Sci. 2012;64:243.
46. Chen W, Luo HQ, Li NB. Corros Sci. 2011; 53:3356.
47. Gojic M. Corros Sci. 2001;43:919.
48. Growcock FB, Jasinski JH. J Electrochem Soc. 1989;136:2310.
49. Macdonald JR, Johanson WB. In: JR Macdonald (Ed.). Theory in impedance spectroscopy. New York:John Wiley& Sons;1987.
50. Lopez DA, Simison SN, de Sanchez SR. Electrochim Acta. 2003;48:845.
51. Stoynov ZB, Grafov BM, Savova-Stoynova B, et al. Electrochemical Impedance. Moscow:Nauka;1991.
52. Singh AK, Quraishi MA. Corros Sci 2010;52:1373.
53. Popova A, Christov M, Vasilev A. Corros Sci. 2007;49:3290.

54. Bentiss F, Lebrini M, Lagrenee M, et al. Electrochim Acta. 2007;52:6865.
55. Popova A, Christov M, Vasilev A. Corros Sci. 2011;53:1770.
56. Khaled KF, Al-Qahtani MM. Mater Chem Phys. 2009;113:150.
57. Bentiss F, Outirite M, Traisnel M, et al. Int J Electrochem Sci. 2012;7:1699.
58. Yuce AO, Kardas G. Corros Sci. 2012;58:86.
59. Lebrini M, Bentiss F, Chihib N, et al. Corros Sci. 2008;50:2914.
60. Kedam M, Mattos OR, Takenouti H. J Electrochem Soc. 1981;128:266.